MHD Equilibria for Plasmas in a Tokamak Engineering Test Reactor (TETR)

T.F. Yang, R.W. Conn, and G.A. Emmert

September 1976

UWFDM-174

FUSION TECHNOLOGY INSTITUTE

UNIVERSITY OF WISCONSIN

MADISON WISCONSIN

MHD Equilibria for Plasmas in a Tokamak Engineering Test Reactor (TETR)

T.F. Yang, R.W. Conn, and G.A. Emmert

Fusion Technology Institute
University of Wisconsin
1500 Engineering Drive
Madison, WI 53706

http://fti.neep.wisc.edu

September 1976

UWFDM-174

UWFDM-174

MHD Equilibria for Plasmas in a Tokamak Engineering Test Reactor (TETR)

T. F. Yang
R. W. Conn
G. A. Emmert

Fusion Technology Program
Nuclear Engineering Department
University of Wisconsin
Madison, Wisconsin 53706

To be published in the Proceedings of the 2nd ANS Topical Meeting - International on The Technology of Controlled Nuclear Fusion, September 21-23, 1976, Richland WA

ACKNOWLEDGEMENTS

This research was supported by grants from the Energy Research and Development Administration and the Wisconsin Electric Utilities Research Foundation.

MHD EQUILIBRIA FOR PLASMAS IN A TOKAMAK ENGINEERING TEST REACTOR (TETR)

T. F. Yang, R. W. Conn, G. A. Emmert

FUSION TECHNOLOGY PROGRAM, UNIVERSITY OF WISCONSIN

The Wisconsin Fusion Design Group is developing a conceptual design of a Tokamak Engineering Test Reactor (TETR). The machine operates in the two-component, beam-driven mode and is designed to produce a high time-averaged neutron wall loading ($\geq$ 1 MW/m^2) for materials testing and blanket studies.[1] In order to achieve this wall loading in a reasonable size device, it is necessary to make the plasma vertically elongated with high poloidal beta and plasma shape factor. Engineering constraints are that the coils be far from the plasma and that there be sufficient access to the sample test area. A series of MHD calculations illustrate that it is difficult to satisfy these constraints simultaneously because the external vertical field acquires the wrong curvature for vertical stability of the plasma column. However, this problem can be circumvented by introducing a feedback stabilization system for the vertical displacement. The plasma design chosen for TETR has a current of 2.52 MA, a major radius of 3.25 m, and an on-axis magnetic field of 42 kG. The average β_θ is 3.8 and q is 2.5 at the plasma edge. The half-width is 0.6 m and the half-height is 1.20 m.

INTRODUCTION

The design goals for a Tokamak Engineering Test Reactor (TETR)[1] are: (1) the average 14 MeV neutron wall loading should be above 1 MW/m^2; (2) the surface heat load on the first wall should simulate wall stresses and surface damage expected in a tokamak reactor, and (3) sufficient space should be available for materials and blanket engineering test modules. One key to the success in designing such a machine lies in finding a MHD equilibrium configuration which can operate with parameters such that sufficient thermonuclear power is released to achieve the design goals. Three primary characteristics, high beta, elongated plasma cross sections, and high toroidal field, are found to be essential. The achievement of a design producing the largest field on axis for a given maximum field at the coil and satisfying constraints posed by blanket and shield design and the desire (an apparent need) for a divertor adds to the difficulty of this problem. A further constraint we have placed ourselves on the TETR design is that it should be a reactor that one could conceive of building in the relatively near term, i.e., the mid-1980's. As such, the engineering of the toroidal and equilibrium field coils should be consistent with this constraint.

The operating mode which yields the highest neutron flux in a tokamak is the neutral beam driven two component approach.[2] This mode requires $n\tau_E$ values of $\sim 10^{13}$ cm^{-3}-sec and typically involves values of both τ_p and τ_E on the order of several hundred milliseconds at most. Long burn times, pumping requirements, plasma protection from impurities, and first wall protection from excessive erosion imply that such devices will require a divertor.

The basic model chosen for this study is a "D" or triangularly shaped plasma that

admits the inclusion of a double null poloidal divertor.[3] The reason is that this shape fills most optimally the available space inside the TF coils. A series of MHD calculations have been carried out, each time iterating the results with plasma performances calculations based on space time fluid simulations and restrictions imposed by the problems associated with neutronics, toroidal field magnets, and access requirements for blanket modules and neutral beam injectors.

Three basic plasma designs were achieved classified as follows: (1) A highly elongated plasma equilibrium that is produced by a set of superconductive coils located outside the blanket and shield but inside the TF coils. The vertical field is such that the plasma is unstable to gross vertical motion. (2) A less elongated and vertically stable plasma with normal coils located inside the blanket. (3) A moderately elongated and mildly unstable plasma equilibrium with different coil arrangements. The results and reasons for our choice are discussed in detail in section III.

II. THE DESCRIPTION OF THE MHD CODE

The MHD equilibrium code developed by a group at the Princeton Plasma Physics Laboratory[4] was used for the equilibrium and local stability calculations. The original code has been modified in several ways, including an addition to calculate the general criteria for stability with respect to rigid motions. The MHD equilibrium for an axisymmetric system is determined by solving the usual equation for the flux function Ψ which satisfies

$$X\frac{\partial}{\partial X}\left(\frac{1}{X}\frac{\partial \Psi}{\partial X}\right) + \frac{\partial^2 \Psi}{\partial Z^2} = -XJ_\phi \qquad (1)$$

where

$$J_\phi = X\frac{dp}{d\Psi} + \frac{R_o^2 B_o^2}{X} g \frac{dg}{d\Psi}. \qquad (2)$$

The magnetic field has been decomposed into poloidal and toroidal components using

$$\vec{B} = B_o[f(\psi)\ \vec{\nabla}\phi X \vec{\nabla}\psi + R_o g(\psi)\vec{\nabla}\phi]. \qquad (3)$$

The coordinates R, ϕ and Z are the axisymmetric coordinates, ϕ is the ignorable variable and X is the distance from the symmetric axis. ψ represents an arbitrary surface label and Ψ is the poloidal flux inside a magnetic surface. The nonlinear equation (1) is solved by prescribing the functions $p(\Psi)$ and $g(\Psi)$ in equation (2). The form employed for the functions $p(\Psi)$ and $g(\Psi)$, used in solving eqn. (1), can have a significant effect on the equilibrium and stability of the plasma. If we choose

$$P(\Psi) = P_o\left(\frac{\Psi_* - \Psi}{\Psi_* - \Psi_o}\right)^{\alpha_1} \qquad (4)$$

and

$$g(\Psi) = \left[1 - g_p\left(\frac{\Psi_* - \Psi}{\Psi_* - \Psi_o}\right)^{\alpha_2}\right], \qquad (5)$$

the plasma current, $j_\phi(\Psi)$, has the form

$$J_\phi(\Psi) = -\frac{XP_o\alpha_1}{\Delta\Psi}\left(\frac{\Psi_*-\Psi}{\Delta\Psi}\right)^{\alpha_1-1} + \frac{\alpha_2 R_o^2 B_o^2}{X\Delta\Psi} g_p \cdot \left(\frac{\Psi_*-\Psi}{\Delta\Psi}\right)^{\alpha_2-1} + \frac{\alpha_2 R_o^2 B_o^2}{X\Delta\Psi} g_p^2 \left(\frac{\Psi_*-\Psi}{\Delta\Psi}\right)^{2\alpha_2-1} \qquad (6)$$

where $\Delta\Psi = \Psi_m - \Psi_*$, and Ψ_*, Ψ_m are the flux at the plasma surface and magnetic axis. The constant g_p is varied until Ψ converges. The current density distribution depends on the parameters, α_1 and α_2. The optimal values of α_1 and α_2 is in the neighborhood of 1.4[5] to give current profile consistent with present tokamak experiments. The plasma boundary is determined self consistently with the location of external coils. A square of arbitrary size is used as an outer boundary for the problem and the boundary conditions on this border are fixed by specifying the current in the external coils. As such, the procedure does not require the use of a conducting external boundary. The plasma boundary can be fixed by a limiter or a separatrix. The program evaluates $q(\Psi)$, $\beta_\theta(\Psi)$ and $\bar{\beta}_\theta$ from the formulae[4,5,6]

$$q(\psi) = \frac{R_o g}{2\pi} \oint \frac{dl}{|\nabla\psi| X} , \quad (7)$$

$$\beta_\theta(\psi) = \frac{2\pi P}{\left\langle \frac{|\nabla\psi|^2}{R^2} \right\rangle} , \quad (8)$$

and

$$\overline{\beta_\theta} = \frac{\int P \frac{dV}{d\psi} d\psi}{\int^\psi P \frac{dV}{d\psi} d\psi - R_o^2 B_o^2 \int^\psi Vg \frac{dg}{d\psi} \left\langle \frac{1}{X^2} \right\rangle d\psi} \quad (9)$$

where V and $\frac{dV}{d\psi}$ are the plasma volume and its derivative with respect to ψ. The total β and average pressure defined respectively as follows.

$$\beta_{total} \cong \frac{\int P \, dV}{\int \frac{B_t^2}{2\mu_o} dV} \quad (10)$$

$$\bar{P} = \frac{\int P \, dV}{\int dV} \quad (11)$$

The criteria for stability with respect to the localized modes are,[7,8] for idealized modes,

$$D_I = D + H - \frac{1}{4} < 0 \quad (12)$$

and for the resistive modes,

$$D_R + D + H^2 < 0 . \quad (13)$$

The parameters D and H are defined by

$$D \equiv \frac{\langle B^2/|\nabla\nabla|^2\rangle}{\Lambda^2} [J'\phi'' - I'\psi'' + \frac{\langle \sigma B^2 \rangle}{\langle B^2 \rangle}$$

$$+ p'^2 \left\langle \frac{1}{B^2} \right\rangle + \left\langle \frac{\sigma^2 B^2}{|\vec{\nabla}\nabla|^2} \right\rangle - \frac{\langle \sigma B^2/|\vec{\nabla}\nabla|^2\rangle^2}{\langle B^2/|\vec{\nabla}\nabla|^2\rangle}] \quad (14)$$

$$H \equiv \frac{\langle B^2/|\vec{\nabla}\nabla|^2\rangle}{\Lambda} \left[\frac{\langle \sigma B^2/|\vec{\nabla}\nabla|^2\rangle}{\langle B^2/|\vec{\nabla}\nabla|^2\rangle} - \frac{\langle \sigma B^2\rangle}{\langle B^2\rangle}\right] \quad (15)$$

where $\Lambda = \phi' \psi'' - \psi' \phi''$ and $\sigma = \vec{J}\cdot\vec{B}/B^2$. ϕ and ψ are the toroidal and poloidal field flux functions and J and I are the toroidal and poloidal current fluxes, respectively. Primes denote derivatives with respect to the volume, V, and brackets denote field line averages.

A new routine has been written and included in this code to compute the general stability criteria related to quasi-rigid motions[5] (vertical and radial displacements and flippings). These modes have been observed experimentally and in many cases can be stabilized by a feedback system.[9] They are actually special kink modes and can be dangerous. In the past, the criterion for determining stability against vertical motion was that the decay index of the vacuum vertical field should be greater than zero.[10] However, this decay index criterion was derived for a circular plasma with uniform current density and large aspect ratio. A noncircular plasma with vertical elongation does not satisfy these restrictions. The general criteria of Rebhan[11] derived using an energy principle for general small rigid displacements will, therefore, be used in this study. The sufficient criteria for horizontal displacement and flipping are, respectively,

$$C_h = \oint \frac{R\psi_R}{|\nabla\psi|} P_R^* d\ell \geq 0 \quad (16)$$

$$C_f = \oint \frac{R(R\psi_z - z\psi_R)}{|\nabla\psi|} (Rp_z^* - zp_R^*) d\ell \geq 0. \quad (17)$$

The necessary and sufficient stability condition for vertical displacements is

$$C_v = \oint \{\frac{1}{R|\nabla\psi|} [-\psi_z\psi_{RR} + \frac{\psi_z\psi_R}{R} + \psi_R\psi_{Rz}] + y\}x$$

$$\psi_z d\ell \geq 0. \quad (18)$$

Here the antisymmetric part of y satisfies the integral function

$$\frac{1}{2\pi} \oint [K(\ell',\ell)y_a - K(\ell,\ell')y_a] d\ell'$$

$$= \frac{1}{2\pi} \oint [L(\ell,\ell')\sigma' - L(\ell',\ell)\sigma] d\ell'. \quad (19)$$

The functions $K(\ell,\ell')$ and $L(\ell,\ell')$ are defined as

$$K(\ell,\ell') = \frac{4R'}{|\nabla\Psi| r_o^3 (1 - k^2)} \{-R'\Psi_R E(k) + \frac{1}{k^2}[R\Psi_R + (z-z')\Psi_z] x [(2 - k^2)E(k) - 2(1-k^2)K(k)]\} \quad (20)$$

and

$$L(\ell,\ell') = \frac{4}{|\nabla\Psi| r_o^3 (1-k^2)} \{[R\Psi_z - (z-z')\Psi_R]E(k) - \frac{R'\Psi_z}{k^2}[(2-k^2)E(k) - 2(1-k^2)K(k)]\} \quad (21)$$

where

$\sigma = [\Psi_z\Psi_{xR} - \Psi_R\Psi_{zz}]/|\nabla\Psi|$, $k = \{4RR'/[(R+R')^2 + (z-z')^2]\}^{1/2}$ and $r_o = 2\sqrt{RR'}/k$. The functions E(k) and K(k) are complete elliptical integrals of the first and second kinds. The general criteria C_h, C_f and C_v have been evaluated numerically using as input the plasma pressure profile and shape generated by MHD equilibrium calculations.[5]

III. RESULTS AND DISCUSSION

The optimal size for TETR has been determined to be a machine with a major radius of about 3 m and a plasma half width of about 0.5 m.[1] The initial plasma current was chosen to be 2.4 MA. The other parameters were B_o = 4.0 T, β_θ = 3.0 and the shape factor, S, the ratio of the plasma circumference to the largest inscribed circle, about 1.8. These parameters will give sufficient power density and are simply estimated from the scaling law

$$P_{nw} \cong 6.15 \times 10^{-4} \left(\frac{B_T}{q_{max}} \frac{S}{A}\right)^4 \beta_\theta^2 \left(\frac{V_p}{A_w}\right) \quad (22)$$

where P_{nw} is the neutron wall loading, B_T is the toroidal field (kgauss), q_{max} is the safety factor at the edge, β_θ is the poloidal beta, V_p is the plasma volume and A_w is the first wall surface area. This formula was obtained using the optimized values of Γ, the fast ion pressure/bulk plasma pressure, and the fusion power gain, Q, by assuming T_e is 5 keV and the neutral beam injection energy is 200 keV.[1] For convenience, we have replaced A_w by the area of the plasma in our survey calculation.

A general decision was made prior to performing any detailed calculations to place the EF coils inside the TF magnets. The reasons are that it is difficult to shape the plasma when the coils are too far away and the currents in these coils would be large, relative even to the plasma current. This would in turn influence the power requirements during start-up and shut-down.

We have investigated two extreme cases in an effort to understand the relationship between plasma MHD equilibrium and stability and various engineering constraints. In the first case, case A, superconducting EF coils are located outside the blanket region. The plasma is highly-elongated at the cost of other problems, such as stability and unusual plasma current profiles. In the second case, case B, normal coils are located as close to the plasma as possible (even within the blanket region.) This provides the most highly elongated yet stable plasma with a reasonable current profile. A comparison of the coil arrangement and plasma shape for both cases is shown in Fig. 1. The pressure and current density profiles are plotted as a function of major radius on the midplane in Fig. 2 and the vacuum equilibrium field is shown in Fig. 3. Table I lists the plasma parameters and power output for both cases.

The criteria for obtaining the solutions are that q (Ψ) should be greater than 1 and that the plasma should satisfy the local stability criteria. Stability with respect to rigid motion is ignored for the time being.

The plasma in case A provides the required neutron power density and wall

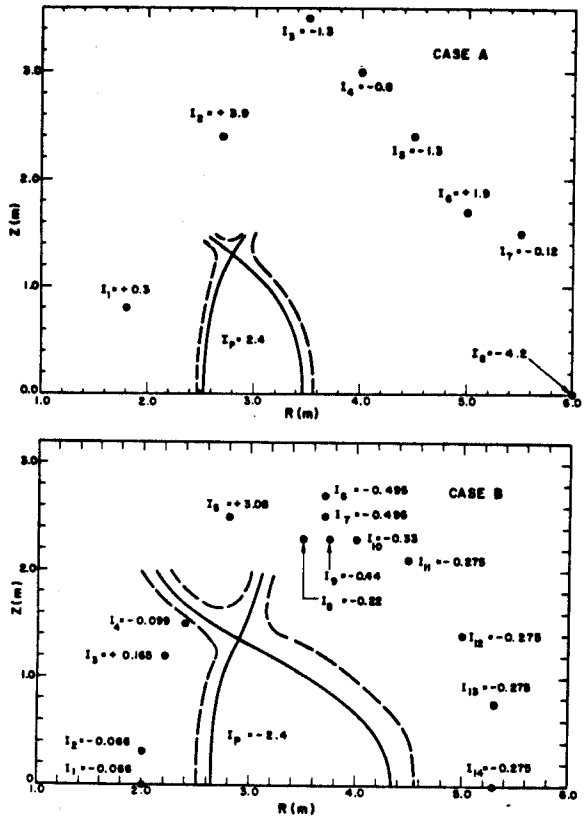

FIGURE 1. Plasma Shapes and External Coil Arrangements for the MHD Equilibria of Cases A and B.

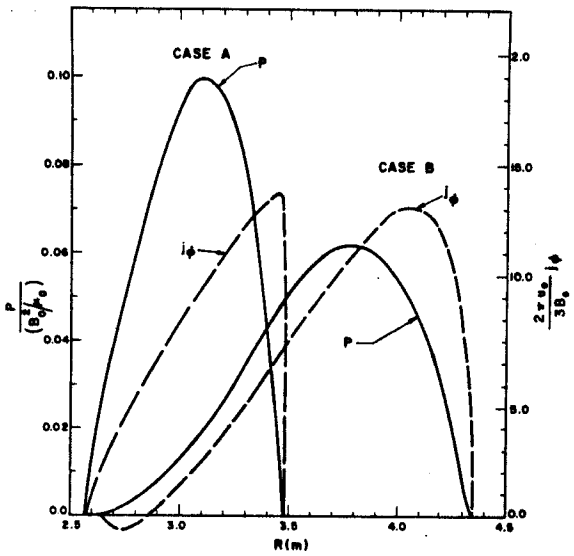

FIGURE 2. Plots of Pressure P (Solid Curves) and Toroidal Current Density (Dashed Curves) for Cases A and B.

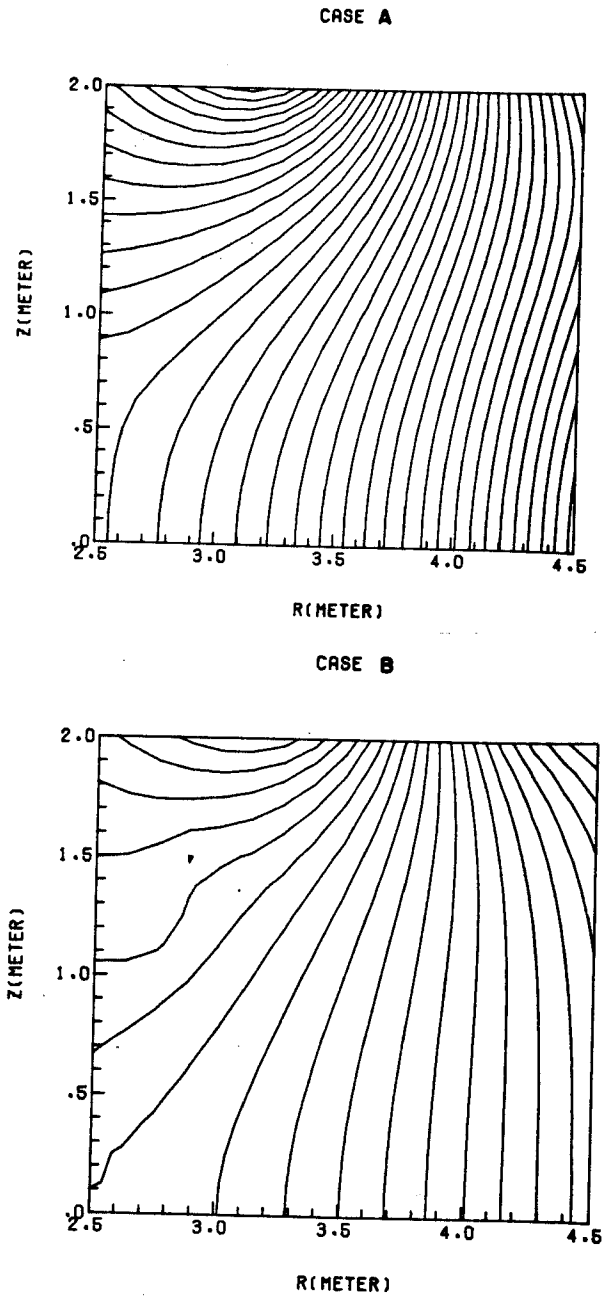

FIGURE 3. Vacuum Vertical Field for Cases A and B.

loading (~1.1 MW/m^2). However, analysis shows this plasma to be highly unstable against the vertical motion and the currents in the superconducting EF coils are very large. Rapid pulsing of such magnets is probably not consistent with the constraint on the TETR design that technologies be reasonably available in the mid-1980's. (This does not imply steady state superconducting toroidal field coils cannot be assumed. Indeed, these should be available given the present magnet development program plans).

TABLE 1. Plasma Parameters for the MHD Equilibrium Cases A and B

	Case A	Case B
I_p(MA)	2.4	2.4
B_T(T)	4.0	4.0
B_{max}(T)	85.0	92.3
Ro(m)	3.0	3.46
Rm(m)	3.1	3.80
b/a	2.75	1.6
a(m)	0.46	0.86
A	6.5	4.1
β_θ	3.5	3.0
S	2.0	1.4
q_{max}	2.6	3.0
A_w(m^2)	109	135
V_p(m^3)	32	74
P_{nw}(MW/m^2)	1.13	0.60

In case B, the plasma elongation is less ($\frac{b}{a}$ = 1.6) and the major radius R_o, and the plasma width, a, are larger than in the previous case. Thus, the reactor is somewhat larger. The coil arrangement has been optimized to give the largest possible elongation consistent with the gross rigid motion stability. (This is possible because the coils are now much closer to the plasma). The currents in the external coils are relatively small (less than 0.5 MA) except for the null-defining coil which is about 3.1 MA. However, this design only produces about 0.5 MW/m^2 for the neutron wall loading, far from the design goal for this machine.

The results from these two extreme cases indicates that one should use normal EF coils and a plasma with intermediate elongation which, when combined with the variation of other parameters such as B_T, β_θ, A and I_p, will produce at least 1 MW/m^2 neutron wall loading.

One obvious possibility is to increase the size of the device to produce greater flexibility but this has the undesirable effects of increasing costs and increasing the volume of the plasma. In turn, this increases the beam power required to maintain the plasma temperature and, overall, is an undesirable solution. We have, therefore, taken the cue from several recent experiments such as Rector and Versator[9] and studied the use of feedback stabilization of the plasma loop. Our analysis shows that plasmas which are mildly unstable against rigid motions can be stabilized with a reasonable feedback system. Thus, we have searched for a mildly unstable plasma equilibrium of smaller size which would nevertheless produce an acceptable neutron wall loading. (By mildly unstable, we mean plasma where the decay index of the vacuum vertical field, $n = -\frac{1}{B_\perp}\frac{dB_\perp}{dr}$, is between 0 and -2). Based on case B summarized in Fig. 1 and Table 1, we have obtained a series of MHD equilibria with different plasma parameters and coil arrangements. Five most typical cases are summarized in Table II. The plasma shapes for cases I and IV are similar and are shown by the solid curve in Fig. 4. The plasma shape for cases II and III are also similar and are indicated by the dashed curve in the same figure. The shaded squares show the arrangement for the external EF coils in case IV.

TABLE II. Plasma Parameters for the MHD Equilibrium Cases I to V

	I	II	III	IV	V
I_p(MA)	2.4	2.4	2.4	2.4	2.4
B_T(T)	4.68	4.68	4.68	4.68	4.68
B_{max}(t)	10.0	10.0	10.0	10.0	10.0
R_o(m)	3.20	3.22	3.22	3.22	3.2
R_m(m)	3.35	3.35	3.35	3.35	3.3
a	0.62	0.65	0.65	0.62	0.62
b/a	2.0	1.9	1.88	2.0	2.0
A	5.2	4.95	4.95	5.1	5.2
β_θ	3.0	3.0	3.0	3.0	3.06
S	1.55	1.40	1.40	1.55	1.55
q_{max}	3.27	3.3	3.28	3.28	2.4
A_w(m^2)	120	125	125	120	118
V_p(m^3)	42.5	45.5	45.5	43.0	42.5
n	-0.85	-0.9	-1.5	-2.0	-2.0
P_{nw}(MW/m^2)	0.6	0.5	0.5	0.7	2.2

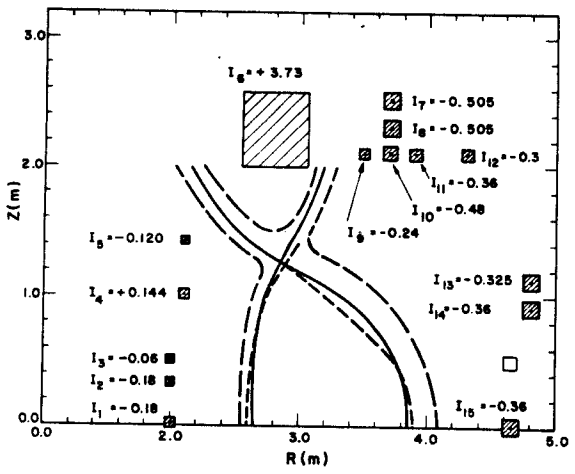

FIGURE 4. The Solid Separatrix is the Plasma Shape for Cases I and IV and the External Coil Arrangement is for Case IV. The Plasma Shape for Case II and III is Shown by the Dashed Separatrix. Cases I-IV are Described in Table II.

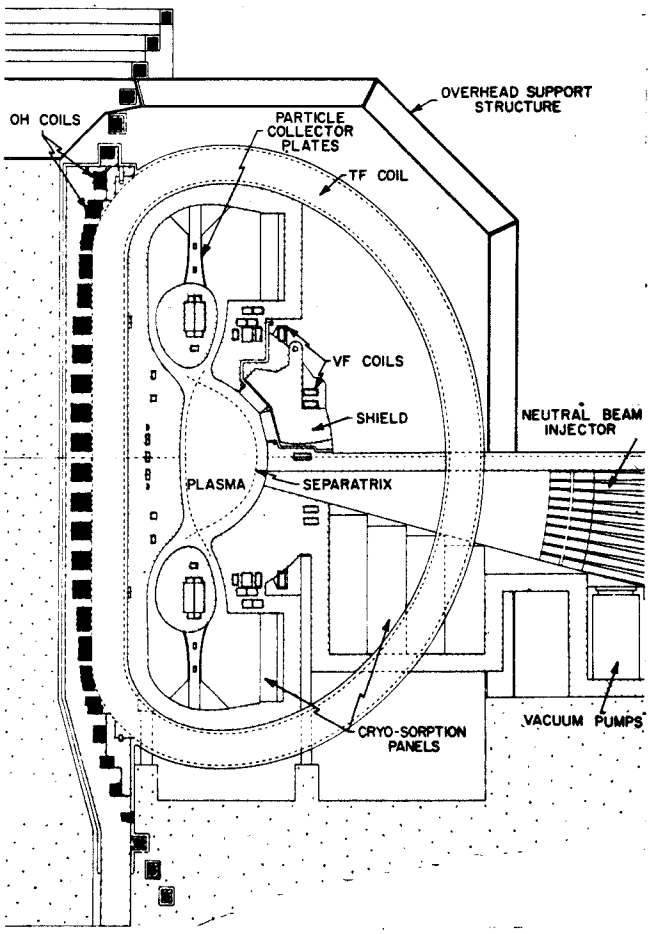

FIGURE 5. Cross Sectional View of Tokamak Engineering Test Reactor (TETR).

All these cases present one or another difficulty. For example, the plasma in case I has a large shape factor, S = 1.55, and a small but negative decay index, n = -0.85. However, because of the presence of EF coils near the midplane, accessibility is poor for beams and test modules. Space for beam and test modules are provided in case IV but to obtain a shape like that in case I, the external midplane coil had to be moved closer to the plasma which left only 85 cm for the blanket and shield. Nevertheless, the beam port can be placed immediately underneath the midplane clear of the coils and shield. The entire space above the midplane is available for test modules. These are shown by the drawing of the cross sectional view of the final design in Fig. 5.

The plasma parameters for the four cases listed in Table II are similar. The power density and neutron wall loading cannot be increased simply by increasing B_T and S because q and A will increase such that the ratio $(\frac{B_T}{q_{max}} \frac{S}{A})$ changes little.

In case V, the plasma current has been raised to 2.9 MA with $q_{max} = 2.4$. The wall loading is now 2.2 MW/m^2 while the EF coil arrangement is the same as for case IV except that the coils carry slightly different currents. Note that in all cases, the maximum field is 10 T and the on-axis field is 4.68 T.

Design number 5 in Table II would meet the goal of the proposed TETR machine if the technology for building 10 T superconducting coil can be presumed for the mid-1980's. This may prove feasible and would ease the problems of developing a high neutron flux machine for either TETR or a tokamak hybrid application. We have taken as a base case the design of a device with a maximum toroidal field of 8.5 T. To meet this stringent constraint, the inner leg of the TF coil is moved outward 10 cm

TABLE III. Plasma Parameters for TETR

R_o = 3.25 m	B_T = 41.9 Kgauss
R_m = 3.37 m	B_{max} = 85 Kgauss
R_{in} = 2.65 m	(at R = 1.60 m)
R_{out} = 3.85 m	β_θ = 3.8
a = 0.6	q_o = 0.95
b = 1.20	q_{max} = 2.5
b/a = 2.0	I_p = 2.52 MA
S = 1.53	n = -2.0
A = 5.42	$B_{\perp o}$ = 3.7 Kgauss
V_p = 41.6 m^3	$\bar{p}$ = 0.49x10^{6}joules/m^3
A_w = 115 m^2	β (total) = 0.066

TABLE IV. Equilibrium Field Coil Arrangement

#	Z	R	I(MA)
D1	0.0	2.0	-0.165
D2	0.3	2.0	-0.165
D3	0.5	2.0	-0.055
D4	1.0	2.1	+0.132
D5	1.4	2.1	-0.110
D6	2.3	1.7	-0.132
†D7	3.2	2.8	+0.066
†D8	3.6	2.8	+0.066
*D9	1.85	2.8	+0.186
*D10	2.1	2.8	+0.477
*D11	2.2	2.8	+0.477
*D12	2.3	2.8	+0.477
*D13	2.4	2.8	+0.477
*D14	2.5	2.8	+0.477
*D15	2.6	2.8	+0.477
*D16	2.7	2.8	+0.239
D17	2.3	3.7	-0.462
D18	2.1	3.7	-0.440
D19	2.5	3.8	-0.473
D20	2.1	3.5	-0.220
D21	2.1	3.9	-0.330
D22	2.1	4.3	-0.275
D23	1.1	4.8	-0.297
D24	0.9	4.8	-0.330
D25	0.0	4.65	-0.330

compared to the previous cases. Then with B_{max} = 8.5 T, B_T on axis is reasonably high, 4.2 T. In addition, I_p has been reduced while keeping q_{max} at about 2.5 to yield a higher β_θ. To compensate the loss of space, the distance between the first wall and the plasma on the inside is only 10 cm. The final value of β_θ is 3.8 and the total β is 0.066, quite reasonable values. There may be some local transport activity near

the magnetic axis due to MHD effects because q is less than 1 there. However, the $n\tau_E$ requirement is not large in a two component device so low q operation should be acceptable. The final TETR plasma design is summarized in Table III and Table IV contains a list of the poloidal field coils. The plot of the surfaces on constant Ψ is shown by Fig. 6. A perspective of the pressure and current profiles are presented in Figs. 7 and 8, respectively, while the vacuum vertical field is shown by Fig. 9. Stabilization of the vertical instability by a feedback system is required and, as

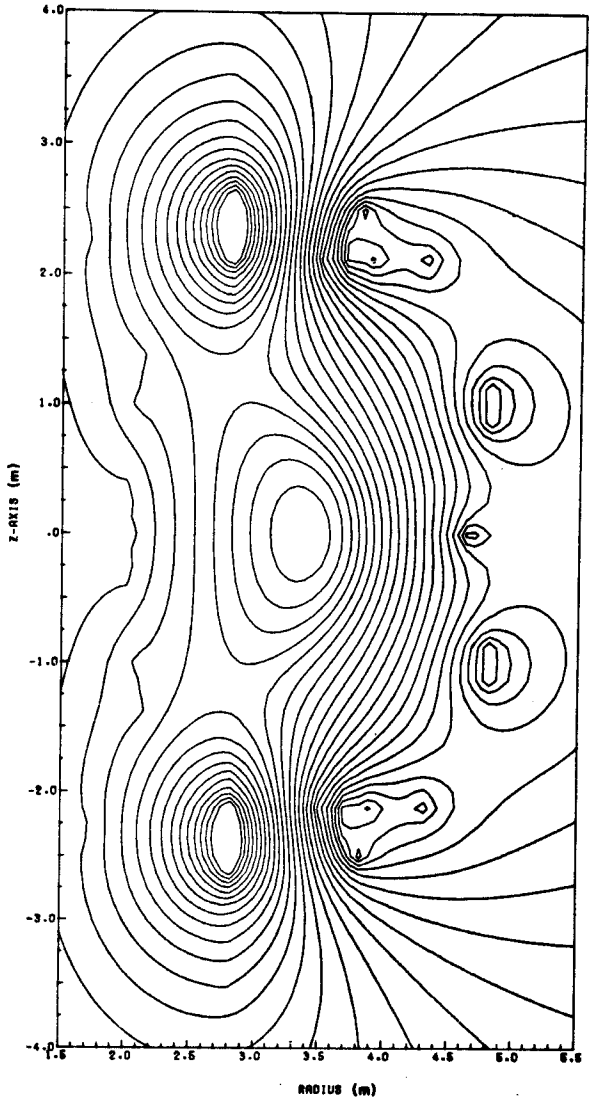

FIGURE 6. Surfaces on Constant Ψ for the Tokamak Engineering Test Reactor (TETR).

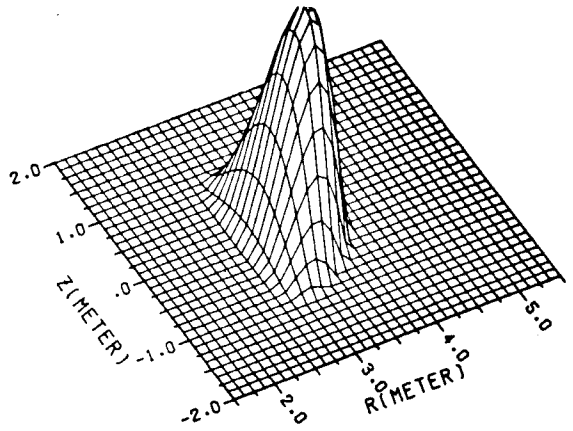

FIGURE 7. Perspective View of the Pressure Profile for TETR.

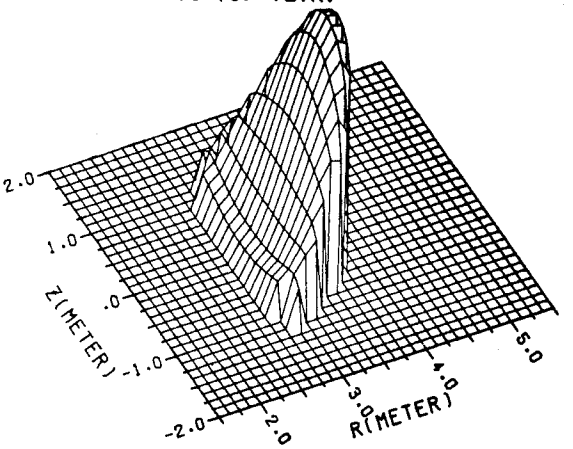

FIGURE 8. Perspective View of the Current Density Distribution for TETR.

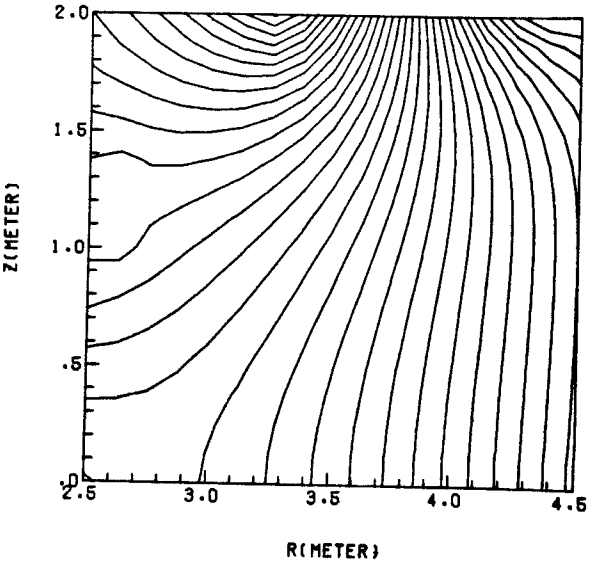

FIGURE 9. Vacuum Vertical Field In TETR.

mentioned, experience on several experiments indicates this to be feasible. For construction reasons, the null-defining coil is split into six coils on top of one another, as indicated by asterisks in Tabie IV. Three additional coils (indicated by a †) are added to spread the field lines near the separatrix at the top of the divertor to lower the particle power density and ease the particle collection problem in the divertor.

IV. CONCLUSIONS

An optimized system of poloidal field coils has been developed for a small, high power density tokamak device which will produce an elongated "D" shaped MHD equilibrium plasma with a current of 2.52 MA, an axial toroidal field of 4.2 T, a shape factor of 1.54 at a poloidal β of 3.8. The aspect ratio is 5.4. This system can produce sufficient power to generate neutron wall loadings above 1 MW/m^2 and has ready accessibility to meet the design goals of TETR. A feedback stabilization system based on the existing EF coils is required to provide overall vertical stability of the current loop.

REFERENCES

1. R. W. Conn and D. L. Jassby, "A Tokamak Engineering Test Reactor," in Proc. International Conf. on Radiation Test Facilities for the CTR Surface and Materials Program (Argonne National Laboratory, ANL/CTR-75-4, 1975) p. 592-624. Also UWFDM-119, University of Wisconsin and MATT-1155, Princeton Plasma Physic Laboratory Report (July 1975).
2. J. M. Dawson, H. P. Furth, F. H. Tenney, Phys. Rev. Lett., 26 1156 (1971). See also H. P. Furth and D. L. Jassby, Phys. Rev. Lett., 32, 1176 (1974).
3. B. Badger et al., "UWMAK-II , A Wisconsin Toroidal Fusion Reactor Design," UWFDM-68, Nuclear Engineering Dept., Univ. of Wisconsin (Nov. 1973), Vol. 1.
4. M. S. Chance et al., Proc. 5th IAEA Conf. on Plasma Physics and Conf. Nucl. Fus. Research, 1974 (IAEA, Vienna, 1975) Vol. I, p. 463.
5. T. F. Yang and R. W. Conn, "Computational Study of MHD Equilibrium on Non-Circular Tokamak Reactor Plasma," to be published in IEEE Trans. on Plasma Science.
6. L. E. Zakharos and V. D. Shafranov, Sov. Phys. Tech. Phys. 18, 151 (1973).
7. J. L. Johnson, J. M. Greene, Plasma Physics 9, 611 (1975).
8. A. H. Glasser, J. M. Greene, J. L. Johnson, Phys. Fluids 18, 875 (1975).
9. U. Ascoli-Bartoli, et al., 5th IAEA Conf. on Plasma Phys. and Cont. Nucl. Fus. Research, 1974 (IAEA, Vienna, 1975) Vol. I, p. 191.
10. S. Yoshikawa, Phys. Fluids 7, 278 (1964).
11. E. Rebhan, Nuclear Fusion 15, 277 (1975).